D^3: Abnormal Driving Behaviors Detection and Identification Using Smartphone Sensors

Zhongyang Chen*, Jiadi Yu*‡, Yanmin Zhu*, Yingying Chen† and Minglu Li*

*Department of Computer Science and Engineering, Shanghai Jiao Tong University, Shanghai, P.R.China

Email: {wodoo2474, jiadiyu, yzhu, mlli}@sjtu.edu.cn

†Department of Electrical and Computer Engineering, Stevens Institute of Technology, Hoboken, USA

Email: yingying.chen@stevens.edu

‡Corresponding Author

Abstract—**Real-time abnormal driving behaviors monitoring is a corner stone to improving driving safety. Existing works on driving behaviors monitoring using smartphones only provide a coarse-grained result, i.e. distinguishing abnormal driving behaviors from normal ones. To improve drivers' awareness of their driving habits so as to prevent potential car accidents, we need to consider a fine-grained monitoring approach, which not only detects abnormal driving behaviors but also identifies specific types of abnormal driving behaviors, i.e. *Weaving*, *Swerving*, *Sideslipping*, *Fast U-turn*, *Turning with a wide radius* and *Sudden braking*. Through empirical studies of the 6-month driving traces collected from real driving environments, we find that all of the six types of driving behaviors have their unique patterns on acceleration and orientation. Recognizing this observation, we further propose a fine-grained abnormal _D_riving behavior _D_etection and i_D_entification system, D^3, to perform real-time high-accurate abnormal driving behaviors monitoring using smartphone sensors. By extracting unique features from readings of smartphones' accelerometer and orientation sensor, we first identify sixteen representative features to capture the patterns of driving behaviors. Then, a machine learning method, *Support Vector Machine* (SVM), is employed to train the features and output a classifier model which conducts fine-grained identification. From results of extensive experiments with 20 volunteers driving for another 4 months in real driving environments, we show that D^3 achieves an average total accuracy of 95.36%.**

I. INTRODUCTION

According to the statistics from World Health Organization (WHO), traffic accidents have become one of the top 10 leading causes of death in the world[1]. Specifically, traffic accidents claimed nearly 3500 lives each day in 2014. Studies show that most traffic accidents are caused by human factors, e.g. drivers' abnormal driving behaviors [2]. Therefore, it is necessary to detect drivers' abnormal driving behaviors to alert the drivers or report Transportation Bureau to record them.

Although there has been works[3][4][5] on abnormal driving behaviors detection, the focus is on detecting driver's status based on pre-deployed infrastructure, such as alcohol sensor, infrared sensor and cameras, which incur high installation cost. Since smartphones have received increasing popularities over the recent years and blended into our daily lives, more and more smartphone-based vehicular applications[6][7][8] are developed in Intelligent Transportation System. Driving behavior analysis is also a popular direction of smartphone-based vehicular ap-
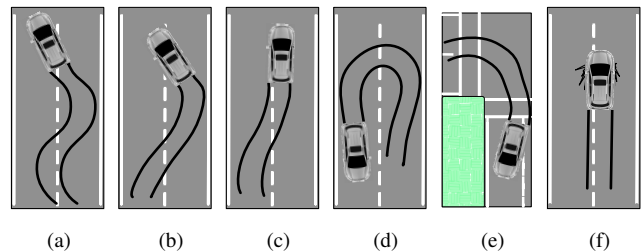

Fig. 1: Six types of abnormal driving behaviors: (a) Weaving, (b) Swerving, (c) Sideslipping, (d) Fast U-turn, (e) Turning with a wide radius, (f) Sudden braking.

plications. However, existing works[9][10] on driving behaviors detection using smartphones can only provide a coarse-grained result using thresholds, i.e. distinguishing abnormal driving behaviors from normal ones. Since thresholds may be affected by car type and sensors' sensitivity, they cannot accurately distinguish the differences in various driving behavioral patterns. Therefore, Those solutions cannot provide fine-grained identification, i.e. identifying specific types of driving behaviors.

Moving along this direction, we need to consider a fine-grained abnormal driving behaviors monitoring approach using smartphone sensors without requiring any additional hardwares. The fine-grained abnormal driving behaviors monitoring is able to improve drivers' awareness of their driving habits as most of the drivers are over-confident and not aware of their reckless driving habits. Additionally, some abnormal driving behaviors are unapparent and easy to be ignored by drivers. If we can identify drivers' abnormal driving behaviors automatically, the drivers can be aware of their bad driving habits, so that they can correct them, helping to prevent potential car accidents. Furthermore, if the results of the monitoring could be passed back to a central server, they could be used by the police to detect drunken-driving automatically or Vehicle Insurance Company to analyze the policyholders' driving habits.

According to [11], there are six types of abnormal driving behaviors defined, and they are illustrated in Fig.1. *Weaving* (Fig.1(a)) is driving alternately toward one side of the lane and then the other, i.e. serpentine driving or driving in S-shape; *Swerving* (Fig.1(b)) is making an abrupt redirection when driving along a generally straight course; *Sideslipping* (Fig.1(c))

1

is when driving in a generally straight line, but deviating from the normal driving direction; *Fast U-turn* (Fig.1(d)) is a fast turning in U-shape, i.e. turning round (180 degrees) quickly and then driving along the opposite direction; *Turning with a wide radius* (Fig.2(e)) is turning cross an intersection at such an extremely high speed that the car would drive along a curve with a big radius, and the vehicle sometimes appears to drift outside of the lane, or into another line; *Sudden braking* (Fig.2(f)) is when the driver slams on the brake and the vehicle's speed falls down sharply in a very short period of time.

This work uses smartphone sensing and machine learning techniques. By extracting unique features from the readings of smartphone sensors, we can detect and identify the six types of abnormal driving behaviors above. To realize a fine-grained abnormal driving behaviors monitoring, we face the following great challenges. First, patterns of driving behaviors need to be identified from readings of smartphone sensors. Second, the noise of smartphone sensors' readings should be removed. Finally, the solution should be lightweight and computational feasible on smartphones.

In this paper, we first set out to investigate effective features from smartphone sensors' readings that are able to depict each type of abnormal driving behavior. Through empirical studies of the 6-month driving traces collected from smartphone sensors of 20 drivers in a real driving environment, we find that each type of abnormal driving behaviors has its unique patterns on readings from accelerometers and orientation sensors. Effective features thus can be extracted to capture the patterns of abnormal driving behaviors. Then, we train those features through a machine learning method, *Support Vector Machine* (SVM), to generate a classifier model which could clearly identify each of driving behaviors. Based on the classifier model, we propose an abnormal *D*riving behaviors *D*etection and i*D*entification system, D^3, which can realize a fine-grained abnormal driving behaviors monitoring in real-time using smartphone sensors. Our prototype implementation of D^3 on Android-based mobile devices verifies the feasibility of using D^3 in real driving environments.

We highlight our main contributions as follows:

- We identify sixteen representative features to capture the patterns of abnormal driving behaviors by empirically analyzing the 6-month driving traces collected from real driving environments.
- We use a machine learning method, SVM, to train the features of driving behaviors and obtain a classifier model which can not only distinguish abnormal driving behaviors from normal ones but also identify specific types of abnormal driving behavior. Machine learning rather than threshold is used in our paper to play down the impact caused by car type or sensor's sensitivity.
- We propose a fine-grained abnormal driving behaviors monitoring system, D^3, to perform real-time high-accurate abnormal driving behaviors detection and identification using smartphone sensors. The fine-grained system can inform drivers of their abnormal driving behaviors which otherwise may be ignored by them so as to improve their awareness

of driving habits.
- We conduct extensive experiments in real driving environments. The result shows that D^3 can identify specific types of abnormal driving behaviors in real time with an average total accuracy of 95.36%.

The rest of the paper is organized as follows: The related work is reviewed in Section II. In Section III, we analyze the acceleration and orientation patterns of the six specific types of abnormal driving behaviors. We present the design details of D^3 in Section IV. We evaluate the performance of D^3 and present the results in Section V. Finally, we give the conclusion remarks in Section VI.

II. RELATED WORK

In this section, we review the existing works on driving behaviors detection, which can be categorized as follows.

Detection using pre-deployed infrastructure: [3] uses an EGG equipment which samples the driver's EGG signals to detect drowsiness during car driving. [12] uses infrared sensors monitoring the driver's head movement to detect drowsy driving. [13] captures the driver's facial images using a camera to detect whether the driver is drowsy driving by image processing. In [4], GPS, cameras, alcohol sensor and accelerometer sensor are used to detect driver's status of drunk, fatigued, or reckless. However, the solutions all rely on pre-deployed infrastructures and additional hardwares that incur installation cost. Moreover, those additional hardwares could suffer the difference of day and night, bad weather condition and high maintenance cost.

Detection using smartphone sensors: To eliminate the need of pre-deployed infrastructures and additional hardwares, recent studies concentrate on using smartphones to detect abnormal driving behaviors. In particular, [14] uses accelerometers, magnetometers and GPS sensors to determine whether high-risk motorcycle maneuvers or accidents occur. [15] uses accelerometers, gyroscopes and magnetometers to estimate a driver's driving style as *Safe* or *Unsafe*. [9][10] use accelerometers to detect drunk driving and sudden driving maneuver, respectively. The works are similar in that they perform a coarse-grained driving behavior detection which uses some thresholds to find out abnormal driving behaviors. Nevertheless, thresholds may be affected by car type and sensors' sensitivity so that they cannot accurately distinguish the differences in various driving behavioral patterns. Therefore, none of existing works can realize fine-grained identification.

III. DRIVING BEHAVIOR CHARACTERIZATION

In this section, we first describe the data collection process for driving behavior samples from real driving environments. Then we analyze patterns of each type of driving behavior from smartphone sensors' readings.

A. Collecting Data from Smartphone Sensors

We develop an Andriod-based App to collect readings from the 3-axis accelerometer and the 3-axis orientation sensor. We align the two coordinate systems in the smartphone and in the vehicle by making the accelerometer's y-axis along the
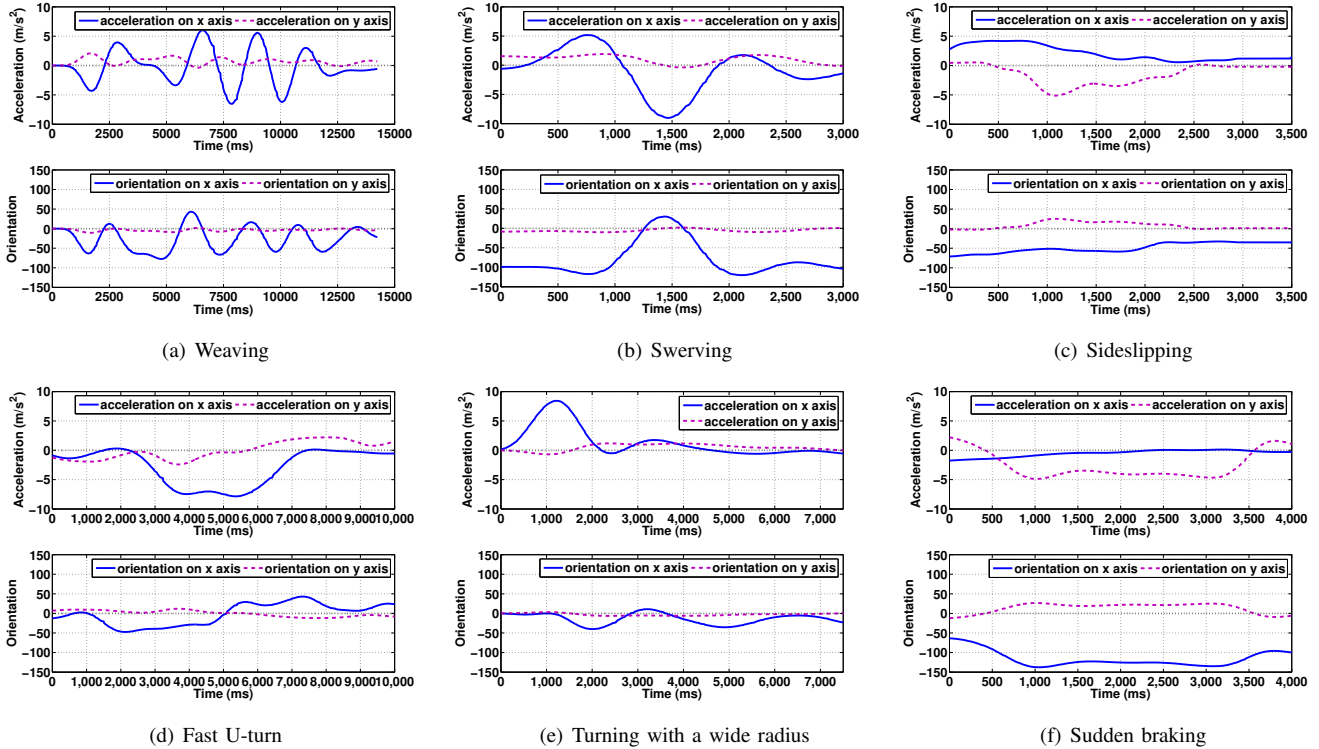
2

Fig. 2: The acceleration and orientation patterns of the six types of abnormal driving behaviors from an accelerometer and an orientation sensor's readings.

moving direction of the vehicle. Therefore, we could monitor the vehicle's acceleration and orientation by retrieving readings from the smartphone's accelerometer and orientation sensor.

We collect traces from the accelerometers and orientation sensors' readings on 20 drivers with distinct vehicles from Jan. 11 to July 12, 2014. Each driver fixes a smartphone along with a Car Digital Video Recorder (DVR) in his/her vehicle within daily natural driving. The smartphone and Car DVR record the sensors' readings and all objective driving behaviors, respectively. The 20 drivers keep collecting data in their daily driving, including commute to work, shopping, touring and so on. Those 20 drivers live in different communities and they have different commute routes. On average, each driver may drive 60 to 80 kilometers per day. 20 smartphones of 5 different types are used in our data collection, i.e. Huawei Honor3C, ZTE U809, SAMSUNG Nexus3, SAMSUNG Nexus4 and HTC sprint, four devices for each type. After that, we ask 9 experienced drivers to watch the videos recorded by the Car DVR and recognize all types of abnormal driving behaviors from the 6-month traces, i.e. *Weaving*, *Swerving*, *Sideslipping*, *Fast U-turn*, *Turning with a wide radius* or *Sudden braking*. In total, we obtain 4029 samples of abnormal driving behaviors from the collected traces, which is viewed as the ground truth.

B. Analyzing Patterns of Abnormal Driving Behaviors

After high frequency noises are removed in the collected data using the low-pass filter, we can analyze the acceleration and orientation patterns of each type of abnormal driving behaviors. Let acc_x and acc_y be the acceleration on x-axis and y-axis,

respectively. Let ori_x and ori_y be the orientation on x-axis and y-axis, respectively.

1) Weaving: Fig.2(a) shows the acceleration and orientation patterns of weaving from an accelerometer and orientation sensor's readings. We observe from this figure that there is a drastic fluctuation on acc_x and this fluctuation continues for a period of time, while acc_y keeps smooth. Thus, both the standard deviation and the range of acc_x are very large and the time duration is long. The mean value of acc_x is around zero. In addition, the orientation values have similar patterns as acceleration values.

2) Swerving: Fig.2(b) shows the acceleration and orientation patterns of swerving. Since swerving is an abrupt, instant behavior, the time duration is very short. When swerving occurs, there is a great peak on both acc_x and ori_x. Thus, the range and standard deviation of both acc_x and ori_x are large, and the mean value is not near zero. In addition, both acc_y and ori_y are flat during swerving.

3) Sideslipping: Fig.2(c) shows the acceleration and orientation patterns of sideslipping. When sideslipping occurs, acc_y falls down sharply. Thus, the minimum value and mean value of acc_y are negative, and the range of acc_y is large. In addition, acc_x in sideslipping is not near zero. If the vehicle slips toward the right side, acc_x would be around a positive value, while if left, then negative. The mean value of acc_x thus is not near zero. When it comes to orientation, there are no obvious changes. Moreover, since sideslipping is an abrupt driving behavior, the time duration is short.

4) Fast U-turn: Fig.2(d) shows the acceleration and orientation patterns of fast U-turn. When a driver turns right or left fast
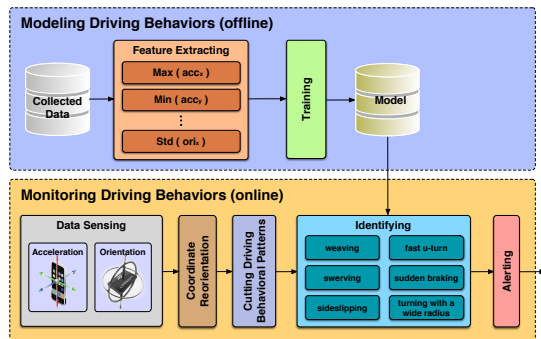
3

Fig. 3: System architecture.

in U-shape, acc_x rises quickly to a very high value or drops fast to a very low value, respectively. Moreover, the value would last for a period of time. The standard deviation of acc_x thus is large on the beginning and ending of a fast U-turn, the mean value of acc_x is far from zero and the range of acc_x is large. When it comes to acc_y, there are no obvious changes. Moreover, ori_x would pass over the zero point. Specifically, ori_x would change either from positive to negative or from negative to positive, depending on the original driving direction. Thus, the standard deviation and value range of ori_x would be large. The mean values in first half and second half of ori_x would be of opposite sign, i.e. one positive and the other negative. It may take a period of time to finish a fast U-turn, so its time duration is long.

5) Turning with a wide radius: The acceleration and orientation patterns of turning with a wide radius are shown in Fig.2(e). When turning at an extremely high speed, acc_x sees a high magnitude for a period of time, while the acc_y is around zero. Thus, the mean value of acc_x is far from zero and the standard deviation of acc_x is large. When it comes to orientation, ori_x sees a fluctuation, while ori_y keeps smooth. The standard deviation of ori_x thus is relatively large, and the mean value of ori_x is not near zero since the driving direction is changed. It may take a period of time to finish a turning with a wide radius, so the time duration is long.

6) Sudden braking: Fig.2(f) shows the acceleration and orientation patterns of sudden braking. When a vehicle brakes suddenly, acc_x remains flat while acc_y sharply downs and keeps negative for some time. Thus, the standard deviation and value range of acc_x are small. On acc_y, the standard deviation is large at the beginning and ending of a sudden braking and the range of acc_y is large. Moreover, there are no obvious changes on both ori_x and ori_y. Since sudden braking is an abrupt driving behavior, the time duration is short.

7) Normal Driving Behavior: Normal driving behavior means smooth and safe driving with few and small fluctuations. Since there are few drastic actions in a normal driving behavior, the values on both acc_x and acc_y are not very large. So the mean, standard deviation, maximum and minimum values in acceleration on x-/y-axis are near zero. When it comes to orientation, a normal driving behavior presents smooth most of time. So the standard deviation and range of orientation are small.

Based on the analysis above, we find that each driving behavior has its unique features, e.g. standard deviation, mean,

maximum, minimum, value range on acc_x, acc_y, ori_x and ori_y, as well as the time duration. Therefore, we could use those features to identify specific types of abnormal driving behaviors using machine learning techniques.

IV. SYSTEM DESIGN

In this section, we present the design of our proposed system, D^3, which detects abnormal driving behaviors from normal ones and identifies different abnormal types using smartphone sensors. D^3 does not depend on any pre-deployed infrastructures and additional hardwares.

A. Overview

In our system, D^3, abnormal driving behaviors could be detected and identified by smartphones according to readings from accelerometers and orientation sensors. Fig.3 shows the architecture of D^3. The whole system is separated into offline part-*Modeling Driving Behaviors* and online part-*Monitoring Driving Behaviors*.

In the offline part, *Modeling Driving Behaviors*, D^3 trains a classifier model using machine learning techniques based on the collected data, which could identify specific types of driving behaviors. In the *Feature Extracting*, effective features are extracted from specific types of driving behavioral patterns on acceleration and orientation. Afterwards, the features are trained in the *Training* and a classifier model would be generated which can realize fine-grained identification. Finally, the classifier model is output and stored to *Model Database*.

The online part, *Monitoring Driving Behaviors*, is installed on smartphones which senses real-time vehicular dynamics to detect and identify abnormal driving behaviors. D^3 first senses the vehicles' acceleration and orientation by smartphone sensors. After getting real-time readings from the accelerometer and the orientation sensor, the *Coordinate Reorientation* is performed to align the smartphone's coordinate system with the vehicle's using the method in [6][7]. Then, in the *Cutting Driving Behavioral Patterns*, the beginning and ending of a driving behavior are found out from accelerometer and orientation sensor's readings. Afterwards, in *Identifying*, D^3 extracts features from patterns of the driving behaviors, then identifies whether one of the abnormal driving behaviors occurs based on the classifier model trained in *Modeling Driving Behaviors*. Finally, if any of the abnormal driving behaviors were identified, a warning message would be sent to receivers by the *Alerting*.

B. Extracting and Selecting Effective Features

In D^3, we use machine learning techniques to identify fine-grained abnormal driving behaviors. The process of feature extraction and selection is discussed in the following.

1) Feature Extraction: When machine learning algorithms are processed, representative tuple of features rather than raw data is a more effective input. Thus, it is necessary to extract effective features from driving behavioral patterns. According to the analysis in Section III, each driving behavior has its unique patterns on acc_x, acc_y, ori_x, ori_y and time duration (t). The main difference between various driving behaviors lies in the

4

(a) Normal vs. Abnormal

(b) Weaving vs. Swerving

(c) Weaving vs. Sideslipping

(d) Weaving vs. Fast U-turn

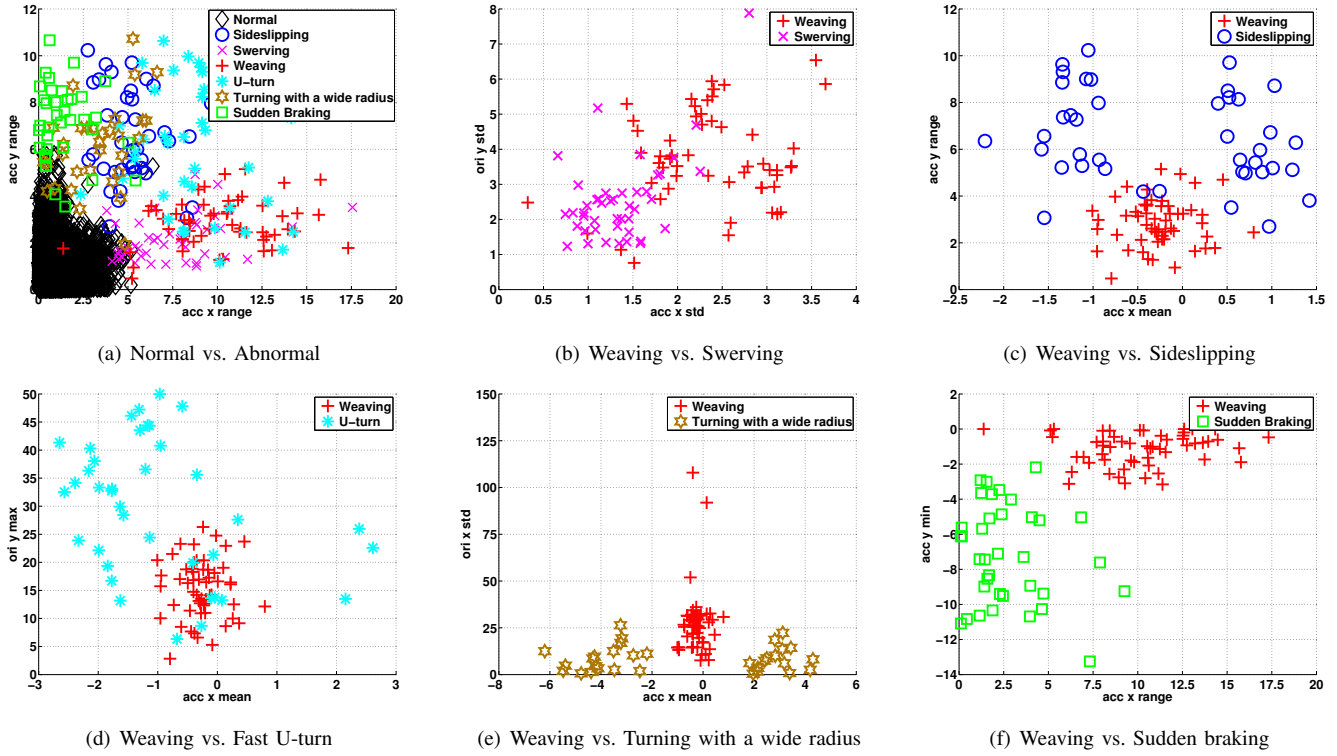(e) Weaving vs. Turning with a wide radius

(f) Weaving vs. Sudden braking

Fig. 4: Some effective features for identifying normal driving behavior from abnormal ones and weaving behavior from other five abnormal driving behaviors.

maximum, minimum, value range, mean, and standard deviation of acc_x, acc_y, ori_x and ori_y and t. Therefore, those values can be used as features for training. However, not all of them are equally effective for abnormal driving behaviors' detection and identification.

2) Feature Selection: In order to select the really effective features, we analyze the collected traces. Fig.4 shows some of the effective features which distinguish abnormal driving behaviors from normal ones and distinguish weaving from the other five abnormal driving behaviors.

Fig.4(a) shows the difference between normal and abnormal driving behaviors in a 2-dimensional features tuple (i.e. $range_{acc,x}$ and $range_{acc,y}$). It can be seen that the two features can clearly discriminate normal and abnormal driving behaviors. Therefore, we manage to distinguish abnormal driving behaviors from normal ones with only two features.

In fact, additionally to the two features shown in Fig.4(a), some other combinations of a 2-dimensional features tuple (i.e. any 2 out of t, $max_{ori,x}$, $max_{ori,y}$, $\sigma_{ori,x}$, $\sigma_{ori,y}$, $\sigma_{acc,x}$, $range_{acc,x}$, $min_{acc,y}$ and $range_{acc,y}$) also manage to distinguish abnormal driving behaviors from normal ones.

Although we can distinguish abnormal driving behaviors from normal ones using a 2-dimensional features tuple, we fail to differentiate the six types of abnormal behaviors from each other only using 2-dimensional features. As the example shown in Fig.4(a), the six types of abnormal driving behaviors are mixed with each other. Nevertheless, they could be differentiated pairwise with a 2-dimensional features tuple. In other words,

although the six abnormal driving behaviors cannot be differentiated from each other at the same time, any two among them can be differentiated intuitively by a 2-dimensional features tuple. Taking weaving for example (see Fig.4(b) - Fig.4(f)), weaving can be distinguished from the other five abnormal driving behaviors using a 2-dimensional features tuple. For instance, in Fig.4(b), weaving and swerving can be discriminated from each other using $\sigma_{ori,y}$ and $\sigma_{acc,x}$. Similarly, other abnormal driving behaviors can also be pairwise discriminated using 2-dimensional features tuples.

Based on the collected traces, we investigate all possible pairwise cases. In each case, we find out several effective features conductive to distinguishing one driving behavior from another. Finally, we identify sixteen effective features that are able to capture the patterns of different types of abnormal driving behaviors, as listed in TABLE I.

C. Training a Fine-grained Classifier Model to Identify Abnormal Driving Behaviors

After feature extracting, we obtain a tuple of features for each driving behavior. Then a classifier model is trained based on the tuples for all driving behaviors through machine learning techniques [17] to identify various driving behaviors. We use the multi-class *SVM* [18][19] to train the classifier model. For each driving behavior, the input into *SVM* is in the form of <16-dimensional features, label>, where the 16-dimensional features are the tuples obtained from the *Feature Extracting* and the label is the type of the driving behavior.
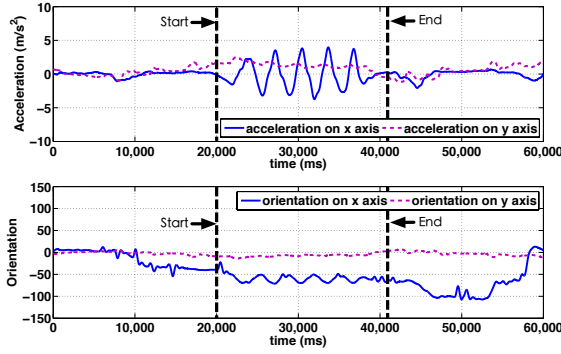
5

Fig. 5: The acceleration and orientation patterns of one minute driving behaviors.

The cores in SVM are the *kernel* and the *similarity function*. A *kernel* is a landmarks, and the *similarity function* computes the similarity between an input example and the kernels. Specifically, assume that our training set contains m samples, and each sample is 16-dimensional (i.e. the 16-dimensional features), denoted by

$$x^{(i)} = (x_1^{(i)}, x_2^{(i)}, \cdots, x_{16}^{(i)}), \qquad i = 1, 2, \cdots, m \quad (1)$$

where $x^{(i)}$ is the i-th sample, and $x_j^{(i)}$ means the j-th feature of $x^{(i)}$. When SVM starts, all input samples $(x^{(1)}, x^{(2)}, \cdots, x^{(m)})$ are selected as kernels, recorded as $l^{(1)}, l^{(2)}, \cdots, l^{(m)}$. Note that $x^{(i)} = l^{(i)}$ for $i = 1, 2, \cdots, m$. Afterwards, for each sample, SVM compute its similarity between the kernels by

$$f_j^{(i)} = e^{-\frac{||x^{(i)} - l^{(j)}||^2}{2\sigma^2}}, \qquad i, j = 1, 2, \cdots, m \quad (2)$$

where $f_j^{(i)}$ is the similarity between input sample $x^{(i)}$ and the kernel $l^{(j)}$, σ is a parameter defined manually, and $||x^{(i)} - l^{(j)}||^2$ is the distance between $x^{(i)}$ and $l^{(j)}$ calculated by

$$||x^{(i)} - l^{(j)}||^2 = \sum_{k=1}^{16}(x_k^{(i)} - l_k^{(j)})^2,$$
$$i, j = 1, 2, \cdots, m \quad (3)$$

In SVM, those m 16-dimensional input samples (i.e. $x^{(1)}, x^{(2)}, \cdots, x^{(m)}$) would be converted into m m-dimentional similarity features (i.e. $f^{(1)}, f^{(2)}, \cdots, f^{(m)}$), since for each $x^{(i)}$, the similarity between $x^{(i)}$ and any $l^{(j)}$ in $l^{(1)}, l^{(2)}, \cdots, l^{(m)}$ are calculated by Equation 2. With the new features $f = (f^{(1)}, f^{(2)}, \cdots, f^{(m)})$, a cost function $J(\theta)$ (see Equation 4) calculated from f would be minimized to find optimal θ.

$$J(\theta) = C \sum_{i=1}^{m} y^{(i)} cost_1(\theta^T f^{(i)}) + (1 - y^{(i)}) cost_0(\theta^T f^{(i)})$$
$$+ \frac{1}{2} \sum_{j=1}^{m} \theta_j^2 \quad (4)$$

where C is a parameter defined manually, $y^{(i)}$ is the label of i-th input example (i.e. the label of $x^{(i)}$), θ^T means θ transpose and

$$cost_1(\theta^T f^{(i)}) = \log(\frac{1}{1 + e^{-\theta^T f^{(i)}}}),$$
$$cost_0(\theta^T f^{(i)}) = \log(1 - \frac{1}{1 + e^{-\theta^T f^{(i)}}}) \quad (5)$$
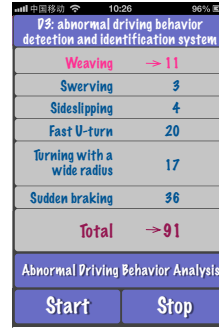

Fig. 6: User interface of D^3 and testbeds.

and

$$\theta^T f^{(i)} = \theta_1 f_1^{(i)} + \theta_2 f_2^{(i)} + \cdots + \theta_m f_m^{(i)} \quad (6)$$

The classifier model would be finally determined by the optimal θ. In a word, *SVM* trains the inputs and then output a classifier model which conducts fine-grained identification to the six types of abnormal driving behaviors.

D. Detecting and Identifying Abnormal Driving Behaviors

After we obtain a classifier model, we are able to detect and identify abnormal driving behaviors in real driving environments using the model. In order to identify current driving behavior using the model, we should input features extracted from patterns of a driving behavior. D^3 thus need to determine the beginning and ending of the driving behavior first, i.e. cutting patterns of the driving behavior. Fig.5 shows the readings from a smartphone' accelerometer and orientation sensor on x-axis and y-axis in a one minute driving, which contains a weaving behavior. In Fig.5, the weaving behavior is sensed from its beginning to ending.

TABLE I: Features Extracted

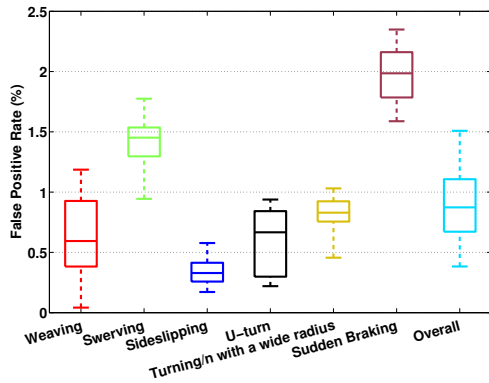| Feature	Description
$range_{acc,x}$	subtraction of maximum minus minimum value of acc_x
$range_{acc,y}$	subtraction of maximum minus minimum value of acc_y
$\sigma_{acc,x}$	standard deviation of acc_x
$\sigma_{acc,y}$	standard deviation of acc_y
$\sigma_{ori,x}$	standard deviation of ori_x
$\sigma_{ori,y}$	standard deviation of ori_y
$\mu_{acc,x}$	mean value of acc_x
$\mu_{acc,y}$	mean value of acc_y
$\mu_{ori,x}$	mean value of ori_x
$\mu_{ori,y}$	mean value of ori_y
$\mu_{acc,x,1}$	mean value of 1st half of acc_x
$\mu_{acc,x,2}$	mean value of 2nd half of acc_x
$max_{ori,x}$	maximum value of ori_x
$max_{ori,y}$	maximum value of ori_y
$min_{acc,y}$	minimum value of acc_y
t	time duration between the begining and the ending of a driving behavior

6

Fig. 7: Box plot of FPR of identifying specific types of driving behaviors.

Fig. 8: Total accuracy under different sizes of training set.

The method of sensing the beginning and ending of a driving behavior is proposed based on an analysis on the acceleration and orientation patterns of all types of driving behaviors. Specifically, when an abnormal driving behavior begins, the standard deviation of either the acceleration or the orientation values sharply rise to and keep a relatively high value until the ending, while in most normal driving behaviors, the standard deviation always presents as low and smooth. Moreover, during an abnormal driving behavior, the magnitude of acceleration on either x-axis or y-axis presents an extremely high value, as illustrated in Section III. But when driving normally, the magnitude of accelerations seldomly reaches to such a high value.

Therefore, It is simple but effective that we monitor the standard deviation of acceleration and orientation as well as the magnitude of acceleration of the vehicle to cut patterns of driving behaviors. In real driving environments, we retrieve readings from smartphones' accelerometers and orientation sensors and then compute their standard deviation as well as mean value in a small window. Under normal driving, D^3 compares the standard deviation and the mean value with some thresholds to determine whether an abnormal driving behavior begins. The window size and thresholds can be learned from the collected data. After the beginning of a driving behavior is found out, D^3 continues to check the standard deviation and mean value to determine whether the driving behavior ends.

After cutting patterns of a driving behavior, effective features can be extracted from the driving behavioral patterns and then sent to the classifier model. Finally, the model outputs a fine-grained identification result. If the result denotes the normal driving behavior, it is ignored, and if it denotes any one of abnormal driving behaviors, D^3 sends a warning message.

V. EVALUATIONS

In this section, we first present the prototype of D^3, then evaluate the performance of D^3 in real driving environments.

A. Prototype

We implement D^3 as an Android App and install it on smartphones (listed in Section III-A). Fig.6 shows the user interface of D^3 and testbeds in vehicles. D^3 is running by 20 drivers with distinct vehicles in real driving environments to collect the data for evaluation. Meanwhile, Car DVRs are used to record driving behaviors and 9 experienced drivers are asked to recognize abnormal driving behaviors as ground truth. After a 4-month data collection (i.e. July 21 to Nov. 30, 2014, using the same method of collecting data as described in Section III-A), we obtain a test set with 3141 abnormal driving behaviors to evaluate the performance of D^3.

B. Metrics

To evaluate the performance of D^3, we define the following metrics based on the True Positive (TP), True Negative (TN), False Positive (FP) and False Negative (FN).

- **Accuracy**: The probability that the identification of a behavior is the same as the ground truth.

TABLE II: Total accuracy in 20 drivers' experiments

Driver	1	2	3	4	5
Total Accuracy (%)	98.66	96.43	95.29	95.61	97.13
Driver	6	7	8	9	10
Total Accuracy (%)	94.55	97.83	99.07	98.37	92.44
Driver	11	12	13	14	15
Total Accuracy (%)	93.46	96.30	94.02	99.59	91.35
Driver	16	17	18	19	20
Total Accuracy (%)	94.50	92.86	94.68	95.49	95.43

TABLE III: Accuracy evaluation

Behavior	Accuracy(%)	Precision(%)	Recall(%)	FPR(%)
Normal	99.84	98.80	100.00	0.19
Abnormal	94.81	100.00	99.80	0.00
Weaving	98.43	92.55	87.87	0.63
Swerving	97.94	92.29	94.15	1.39
Sideslipping	98.60	87.96	71.43	0.37
Fast U-turn	98.49	85.71	76.00	0.54
Turning with a wide radius	98.68	89.30	92.72	0.86
Sudden braking	95.74	97.88	99.04	1.93

7

Fig. 9: Accuracy under different traffic conditions and rode types.

Fig. 10: CDF of FPR under different smartphone placements.

- **Precision**: The probability that the identifications for behavior A is exactly A in ground truth.
- **Recall**: The probability that all behavior A in ground truth are identified as A.
- **False Positive Rate (FPR)**: the probability that a behavior of type Not A is identified as A.

In the following subsections, we investigate the impact of various factors to D^3 and present the details.

C. Overall Performance

The performance of D^3 is evaluated by 3 levels, i.e. total accuracy, detecting abnormal vs. normal driving behaviors and identifying fine-grained driving behaviors.

1) Total Accuracy: Total accuracy is the ratio of correct identifications to total identifications, containing identifications for the six types of abnormal driving behaviors as well as the normal. The total accuracy for each driver is evaluated respectively in TABLE II. It can be seen that all of the 20 drivers achieve high total accuracies. Among the 20 drivers, the lowest total accuracy is 92.44%. On average, D^3 achieves a total accuracy of 95.36%.

2) Detecting the Abnormal vs. the Normal: In this level, we treat all types of abnormal driving behaviors as one type (i.e. *Abnormal*), and merely identify whether a driving behavior is abnormal or normal. As is shown in TABLE III, D^3 performs so excellent that almost all abnormal driving behaviors are identified, with only 6 out of 3141 omitted. In other words, D^3 could identify abnormal driving behaviors vs. normal ones with a recall of 99.84%. In addition, none of normal driving behaviors is identified as abnormal one, i.e. with 100% precision and 0 FPR.

3) Identifying Abnormal Driving Behaviors: D^3 also realizes fine-grained identification, i.e., discriminates *Weaving*, *Swerving*, *Sideslipping*, *Fast U-turn*, *Turning with a wide radius* and *Sudden braking*. TABLE III shows the identification results. The accuracy for identifying each of the six abnormal driving behaviors is no less than 94%, the precision is above 85%, and the recall is more than 70%. The FPRs for identifying all types of abnormal driving behaviors are no more than 2%. The results show that D^3 is an high-accurate system to identify various abnormal driving behaviors.
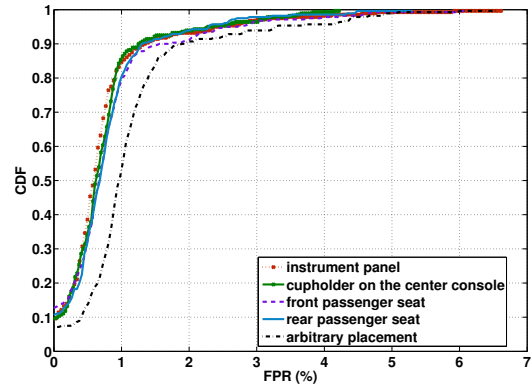
Moreover, we evaluate FPRs of identifying specific abnormal types. Fig.7 shows a box-plot of the FPRs for each type of abnormal driving behaviors and the overall FPR. As is shown in the figure, the highest FPR of identifying specific abnormal type is less than 2.5% and the overall FPR is around 0.9%, which shows that D^3 could implement fine-grained identification with few false alarms. In addition, D^3 performs better when identifying weaving, sideslipping, turning with a wide radius and fast U-turn than identifying swerving and sudden braking. This is because the patterns of the former ones are more distinct than that of the latter. However, the performance of identifying swerving, sideslipping and turning with a wide radius is more stable than identifying other abnormal driving behaviors since they have smaller standard deviations. This is because the patterns of the former ones are more stable than that of the latter.

D. Impact of Training Set Size

According to Section III-A, we collect 4029 abnormal driving behaviors in total for training. The training set size (i.e. the number of training samples) may have an impact on the training results so that it may affect the performance of D^3. We thus evaluate the impact of the training set size. The results are shown in Fig.8. From the figure, we observe that the more training samples there are, the better performance D^3 has. When we use 280 training samples for turning with a wide radius, sideslipping, 300 sudden braking samples, 350 swerving samples and 380 training samples for fast U-turn and weaving, respectively, D^3 could identify each specific type of driving behavior with an accuracy close to 100%. In order to guarantee the performance of D^3, we use as many training samples as possible.

E. Impact of Traffic Conditions

The traffic conditions may affect the drivers' driving behaviors and further affect the performance of D^3. We analyze traces during peak time and off-peak time respectively to evaluate the impact of traffic conditions. Fig.9 shows the accuracies of identifying specific types of abnormal driving behaviors during peak and off-peak time. It can be seen that D^3 achieves good accuracy during both time periods, and the accuracy in off-peak time is slightly higher than that in peak time. This is because during peak time, the vehicles perform less drastic actions due to traffic jams. So some abnormal driving behaviors

8

present restrained patterns during peak time. Different types of abnormal driving behaviors thus are much easier to be mistaken by each other and even be mistaken as normal driving behaviors. Nevertheless, during off-peak time, the patterns of all types of driving behaviors are performed more obvious. So different types of abnormal driving behaviors are more distinguishable.

F. Impact of Road Type

Drivers could perform abnormal driving behaviors on highway or local road, thus we further investigate the impact of the two road types on the performance of D^3. Fig.9 shows how road types affect the accuracy of identifying various types of abnormal driving behaviors. It can be seen that D^3 achieves good accuracy both on highway and local road, but the accuracy is slightly higher on highway than that on local road. This is because the better road condition on highway could reduce the fluctuations caused by bumpy surfaces. Since highway is more smooth and has less slopes compared with local road, there are less disturbances then. In addition, there are less curves and no traffic light stops on the highway, so when driving normally on the highway, drivers have less chance to perform drastic actions. As a result, D^3 can achieve a better performance on highway than that on local road.

G. Impact of Smartphone Placement

Smartphones could be arbitrarily placed in vehicles, we thus investigate the impact of smartphone placement. In our experiments with 20 vehicles, smartphones are fixed on instrument panel, cupholder on the center console, front passenger seat, or left rear passenger seat, where smartphone sensors' y-axis is aligned along the moving direction of vehicles, or on arbitrary placement (i.e. smartphones are put in the driver's pocket and its pose could be arbitrary). Fig.10 shows the CDF of FPRs of fine-grained identifications under different smartphone placements. It can be seen that D^3 can achieve low FPRs under all smartphone placements, which shows D^3 performs excellent wherever the smartphone is placed in a vehicle. Although there is slightly higher FPR under arbitrary placement because of errors in the coordinate reorientation process, a FPR of less than 2% in 90% of the cases is still a good result.

VI. Conclusion

In this paper, we address the problem of performing abnormal driving behaviors detection (coarse-grained) and identification (fine-grained) to improve driving safety. In particular, we propose a system, D^3, to detect and identify specific types of abnormal driving behaviors by sensing the vehicle's acceleration and orientation using smartphone sensors. Compared with existing abnormal driving detection systems, D^3 not only implementes coarse-grained detections but also conducts fine-grained identifications. To identify specific abnormal driving behaviors, D^3 trains a multi-class classifier model through SVM based on the acceleration and orientation patterns of specific types of driving behaviors. To obtain effective training inputs, we extract 16 effective features from driving behavioral patterns collected from the 6-month driving traces in real driving environments. The

extensive experiments driving in real driving environments in another 4 months show that D^3 achieves high accuracy when detecting and identifying abnormal driving behaviors.

References

[1] World.Health.Organisation. The top ten causes of death. [Online]. Available: http://www.who.int/mediacentre/factsheets/fs310/en/

[2] C. Saiprasert and W. Pattara-Atikom, "Smartphone enabled dangerous driving report system," in *Proc. HICSS*, 2013.

[3] M. V. Yeo, X. Li, K. Shen, and E. P. Wilder-Smith, "Can svm be used for automatic eeg detection of drowsiness during car driving?" *Elsevier Safety Science*, vol. 47, pp. 115–124, 2009.

[4] S. Al-Sultan, A. H.Al-Bayatti, and H. Zedan, "Context-aware driver behavior detection system in intelligent transportaion system," *IEEE Trans. on Vehicular Technology*, vol. 62, pp. 4264–4275, 2013.

[5] J. Paefgen, F. Kehr, Y. Zhai, and F. Michahelles, "Driving behavior analysis with smartphones: insights from a controlled field study."

[6] Y. Wang, J. Yang, H. Liu, Y. Chen, M. Gruteser, and R. P. Martin, "Sensing vehicle dynamics for determining driver phone use," in *Proc. ACM MobiSys*, 2013.

[7] H. Han, J. Yu, H. Zhu, Y. Chen, J. Yang, Y. Zhu, G. Xue, and M. Li, "Senspeed: Sensing driving conditions to estimate vehicle speed in urban environments," in *Proc. IEEE INFOCOM*, 2014.

[8] S. Reddy, M. Mun, J. Burke, D. Estrin, M. Hansen, and M. Srivastava, "Using mobile phones to determine transportation modes," *ACM Trans. on Sensor Networks*, vol. 6, no. 13, 2010.

[9] J. Dai, J. Teng, X. Bai, and Z. Shen, "Mobile phone based drunk driving detection," in *Proc. PervasiveHealth*, 2010.

[10] M. Fazeen, B. Gozick, R. Dantu, M. Bhukuiya et al., "Safe driving using mobile phones," *IEEE Trans. on Intelligent Transportation Systems*, vol. 13, pp. 1462–1468, 2012.

[11] U.S.NHTSA. The visual detection of dwi motorists. [Online]. Available: http://www.shippd.org/Alcohol/dwibooklet.pdf

[12] D. Lee, S. Oh, S. Heo, and M. Hahn, "Drowsy driving detection based on the driver's head movement using infrared sensors," in *Proc. IEEE ISUC*, 2008.

[13] M. Kaneda, H. Obara, and T. Nasu, "Adaptability to ambient light changes for drowsy driving detection using image processing," in *JSAE Review*, 1999.

[14] N. Condro, M.-H. Li, and R.-I. Chang, "Motosafe: Active safe system for digital forensics of motorcycle rider with android," *IJIEE*, vol. 2, no. 4, pp. 612–616, 2012.

[15] H. Eren, S. Makinist, E. Akin, and A. Yilmaz, "Estimating driving behavior by a smartphone," in *Proc. IEEE IV*, 2012.

[16] Y. Wang, J. Yang, and Y. Chen, "Tracking human queues using single-point signal monitoring," in *Proc. ACM MobiSys*, 2014.

[17] P. Harrington, *Machine Learning in Action*. Manning Publications, 2012.

[18] Y. Guo, L. Yang, X. Ding, J. Han, and Y. Liu, "Opensesame: Unlocking smart phone through handshaking biometrics," in *Proc. IEEE INFOCOM*, 2013.

[19] C. Chang and C. Lin, "Libsvm: a library for support vector machines," *ACM Trans. on Intelligent Systems and Technology*, vol. 2, no. 3, pp. 1–27, 2011.

[20] H. Han, J. Yu, H. Zhu, Y. Chen, J. Yang, G. Xue, Y. Zhu, and M. Li, "E3: Energy-efficient engine for frame rate adaptation on smartphones," in *Proc. ACM SenSys*, 2013.

9